

## CHAPTER IV

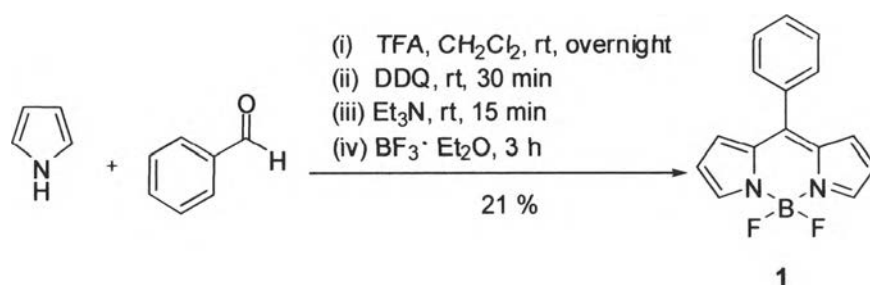
### RESULTS AND DISCUSSION

The hypothesis for the molecular design of the organic photosensitizer in this project is the expansion of the conjugation system of the BODIPY can be achieved by the introduction of (i) the fused benzo ring on the pyrrolic rings and (ii) the thienyl and bithienyl rings into the meso position, leading to the red-shift of absorption and emission peaks. The results from the studies are described as follows.

#### 4.1 Synthesis and characterization

##### 4.1.1 Synthesis and characterization of BODIPY-thiophene derivatives

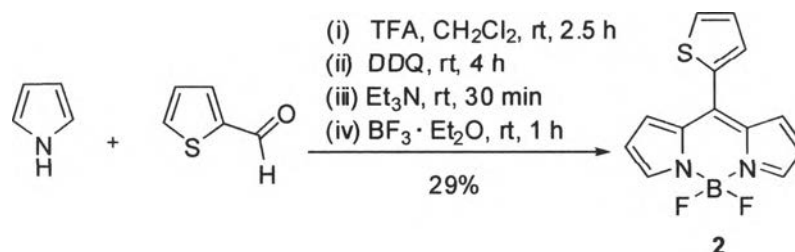
Following a previously published procedure [74], synthesis of BODIPY **1** was achieved by a conventional condensation between pyrrole and benzaldehyde under an acid-catalyzed condition as shown in **Scheme 4-1**. After DDQ-oxidation and subsequent complexation with boron, BODIPY **1** was obtained in 21% yield. In its  $^1\text{H-NMR}$  spectrum (**Figure A-1**), a singlet signal of at 7.95 ppm and a multiplet signal at 7.61–7.50 ppm were observed, indicating the pyrrolic  $\alpha$ -protons and protons on the meso phenyl ring, respectively. Besides, mass spectra also confirmed the formation of BODIPY **1** (**Figure A-2**) by showing its molecular ion peak at  $m/z$  267.399.



**Scheme 4-1:** Synthesis of BODIPY **1**

The synthesis of the target BODIPY **2** relied on a one-pot three-step procedure [71] (**Scheme 4-2**), including (i) TFA-catalyzed condensation of thiophenecarboxaldehyde and pyrrole, (ii) DDQ-oxidation of the resulting dipyrromethane, (iii) quenching of acidic species in the reaction, and (iv) boron complexation of the dipyrin. After purification by column chromatography on silica gel, BODIPY **2** was obtained in 29% yield. High resolution mass spectrum confirmed the formation of BODIPY **2** (**Figure A-5**) by showing its molecular ion peak at  $m/z$

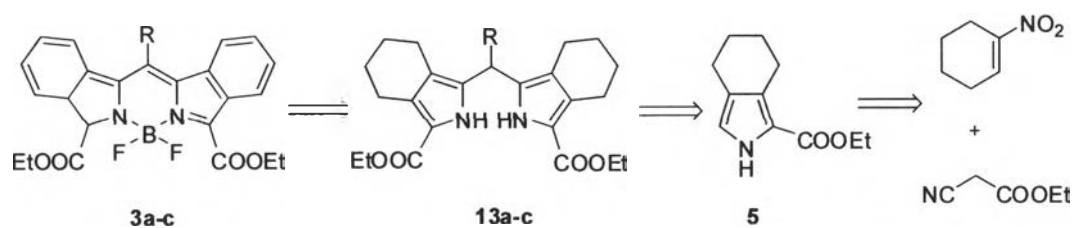
297.0448. According to the  $^1\text{H-NMR}$  spectrum (Figure A-3), a singlet signal of compound **2** at 7.93 ppm and a multiplet signal at 7.25–7.30 ppm were observed, indicating its pyrrolic  $\alpha$ -protons and protons on the meso thieryl ring, respectively.



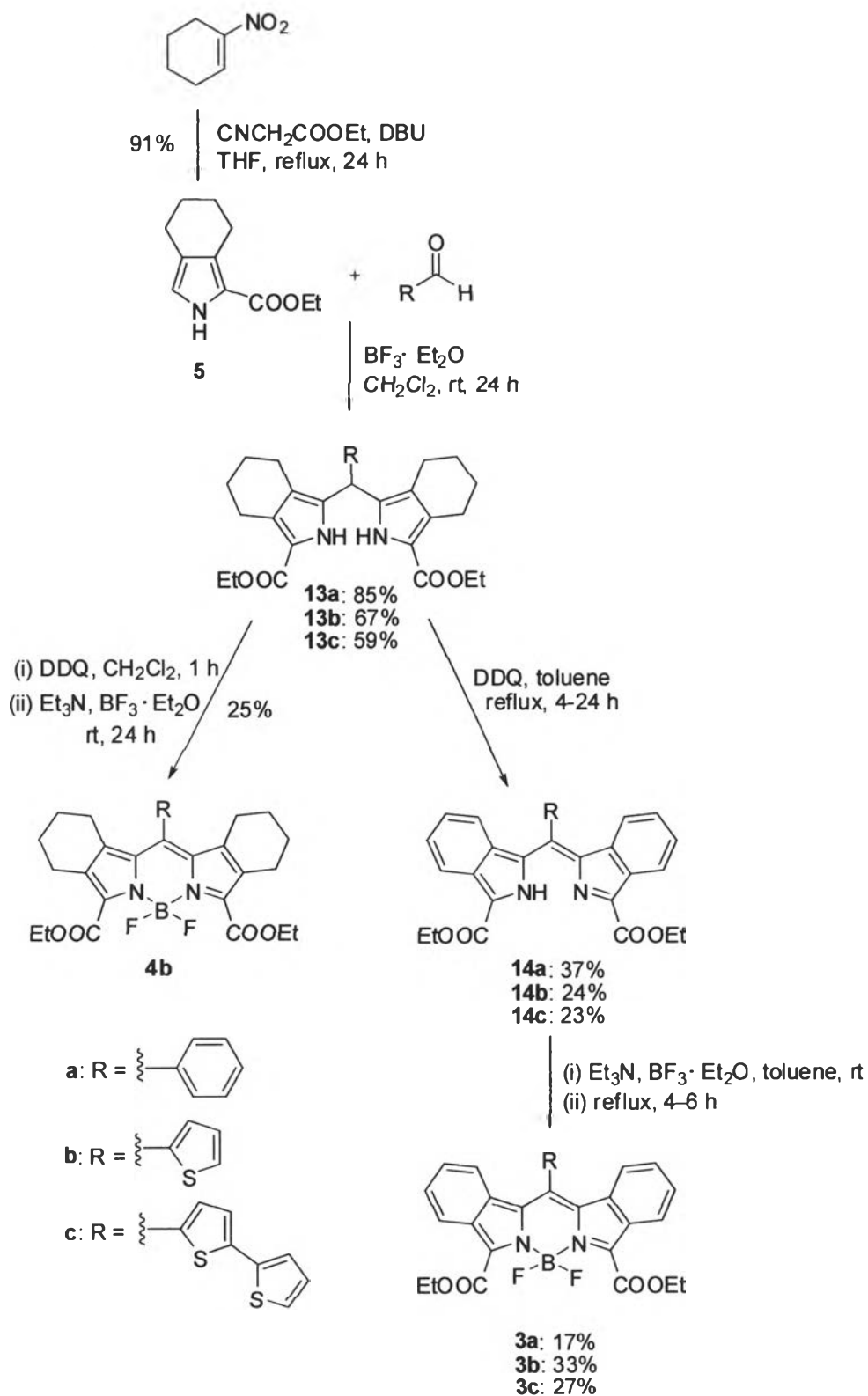
Scheme 4-2: Synthesis of BODIPY **2**

#### 4.1.2 Synthesis and characterization of benzo-BODIPY thiophene derivatives

The structure of target BODIPY **3a-3c** along with the retrosynthetic analysis is depicted in Scheme 4-3, showing that benzo-BODIPYs can be synthesized from thermodynamically stable 4,5,6,7-tetrahydroisindole ester (**5**). The synthesis of benzo-BODIPY derivatives are shown in Scheme 4-4.



Scheme 4-3: Retrosynthetic route of benzo-BODIPYs **3a-c**



Scheme 4-4: Synthesis of benzo-BODIPY derivatives

As a starting material of the entire reaction sequence, 4,5,6,7-tetrahydroisindole ester **5** was prepared in bulk quantities from commercially available 1-nitroarenes and ethyl isocyanoacetate in a presence of DBU via Barton-Zard synthesis [75].

*Meso*-substituted dipyrromethanes **13a-c**, which are the main precursors in this benzo-BODIPY synthesis, were prepared via a one-pot method based on an acid-catalyzed condensation of an appropriate aldehyde with two equivalent of isoindole **5** [73]. This classical approach when applied to the synthesis of dipyrromethane **13a-c** afforded the target compounds **13a-c** in 59–85% yields. All resulting dipyrromethanes were analyzed by  $^1\text{H}$  and  $^{13}\text{C}$ -NMR spectroscopy. A well-resolved  $^1\text{H}$ -NMR spectrum of **13a** (Figure A-18) showed a broad signal of NH protons at 8.50–8.60 ppm, a sharp singlet of the *meso*-proton at 5.40 ppm and a multiplet signal of phenyl protons at 7.09–7.35 ppm. A series of doublet signals indicating 16 protons on two fused-cyclohexenyl rings appeared at 1.58–2.82 ppm. Similarly, a  $^1\text{H}$ -NMR spectrum of **13b** (Figure A-20) showed the broad signal of NH protons at 9.90 ppm, the sharp singlet of the *meso*-proton at 5.69 ppm, and the multiplet signal of the thienyl protons at 6.73–7.16 ppm. A series of the doublet signals indicating of 16 protons on the two fused-cyclohexenyl rings appeared at 1.65–2.83 ppm. Also, a  $^1\text{H}$ -NMR spectrum of **13c** (Figure A-23) showed the broad signal NH protons at 9.91 ppm, the sharp singlet of the *meso*-proton at 5.61 ppm, and the multiplet signal of of thienyl protons at 6.60–7.16 ppm. A series of the doublet signal indicating of 16 protons of the two fused-cyclohexenyl rings appeared at 1.63–2.77 ppm. For all compound **13a-c**, characteristic peak of a formyl group of the starting aldehydes was no longer observed. A small difference in the chemical shifts among all three *meso* substitution on **13a-c** are attributed to the ring current of the *meso*-thienyl group which is roughly perpendicular to the effective indacene plane, leading to deshielding of the  $\alpha$ -protons in the *meso*-substituted area. Dipyrromethanes **13b** (Figure A-22) and **13c** (Figure A-25) gave their  $[\text{M} + \text{Na}]^+$  peaks in the HR-ESI-mass spectra at 503.1975 and 585.1851, respectively.

The synthesis of benzo-BODIPYs **3a-c**, which commenced with the synthesis of dipyrins **14a-c** from dipyrromethanes **13a-c**. Aromatization of **13a-c** into dipyrins **14a-c** was realized by oxidation with 9 equivalents of DDQ in refluxing toluene for 4–24 h. Progress of the reaction was monitored from the change in color of the reaction mixture from orange to purple and by the appearance of the absorption

peak at 574–590 nm. The yields obtained was in a range of 24–37%. The dipyrins **14a-c** (Figure A-27, A-30, A-33) was proven by their  $^1\text{H-NMR}$  spectra, **14a-c** showing the absence of the cyclohexenyl signals at 1.58–2.83 ppm and the presence of additional signals in the aromatic region with the integration of 8 protons. Based on mass spectrometry, BODIPY **14a** (Figure A-29) exhibited a molecular ion peak in its MALDI-TOF-mass spectrum at  $m/z$ : 463.710, while BODIPY **14b** (Figure A-32) and **14c** (Figure A-35) gave their  $[\text{M} + \text{Na}]^+$  peaks in the HR-ESI-mass spectra at  $m/z$ : 493.1202 and 575.1059, respectively.

Reactions of dipyrins **14a-c** with  $\text{BF}_3 \cdot \text{OEt}_2$  in the presence of  $\text{Et}_3\text{N}$  in refluxing toluene for 4–24 h gave rise to the formation of the corresponding benzo-BODIPYs **3a-c** in 17–33% yields. Mass spectrometry analysis showed a molecular ion peak of **3a** (Figure A-8) in MALDI-TOF-mass spectrum at  $m/z$ : 511.842 and HR-ESI-mass spectra analysis exhibited the  $[\text{M} + \text{Na}]^+$  peaks of **3b** (Figure A-11) and **3c** (Figure A-14) at  $m/z$ : 541.1181 and 623.1061, respectively. The  $^1\text{H-NMR}$  spectra of **3a-c** showed 8 protons of the two fused-benzo rings appeared at 6.0–8.5 ppm. Satisfactory solubility of these compounds in various common organic solvents such as  $\text{CH}_2\text{Cl}_2$ ,  $\text{CHCl}_3$ , toluene, THF, etc, showed their usefulness for film preparation in the wet processes.

The attempts to remove the ester groups on the pyrrolic rings following a method described by Y. Tomimori, *et al.* [76] failed to give the ester-free BODIPYs in satisfactory yield due to the complication in the separation step. The compounds **3a-c** were then used for further investigation of the photophysical and electrochemical studies.

BODIPY **4b** was successfully synthesized to compare its photophysical properties with those of benzo-BODIPY **3b**. The BODIPY **4b** was synthesized from dipyrromethane **13b** via a two-step one-flask procedure. In the first step, dipyrromethane **13b** was oxidized with 1.2 equivalents of DDQ in  $\text{CH}_2\text{Cl}_2$  at 0 °C. The progress of the reaction was monitored by TLC analysis, which clearly indicated the formation of corresponding dipyrin as the sole product within 20 minutes. Without isolation, dipyrin was treated with triethylamine (6 equivalents) and  $\text{BF}_3 \cdot \text{OEt}_2$  (10 equivalents). TLC and absorption spectral analysis showed absorbance at 550 nm of the crude reaction mixture, indicating the formation of BODIPY **4b**. The crude product was then subjected to silica gel column chromatographic purification to afford BODIPY **4b** as a pink solid in 25% yield. The formation of BODIPY **4b** (Figure A-17) was confirmed by its  $[\text{M} + \text{Na}]^+$  peak in the HR-ESI-mass spectrum at  $m/z$ :

549.1776. Compared with dipyrromethane **13b**,  $^1\text{H-NMR}$  spectrum of BODIDY **4b** (Figure A-15) exhibited the absence of the signal corresponding to NH protons at 9.90 ppm due to the boron-complexation and the absence of the sharp singlet of the *meso*-proton at 5.69 ppm.

#### 4.2 Investigation of photophysical properties

The structures in this research were shown in Chart 4-1. The photophysical properties of BODIPYs **1-4**, dipyrins **14a-c** and BODIPY **15** were investigated in toluene. The results are summarized in Table 4-1.

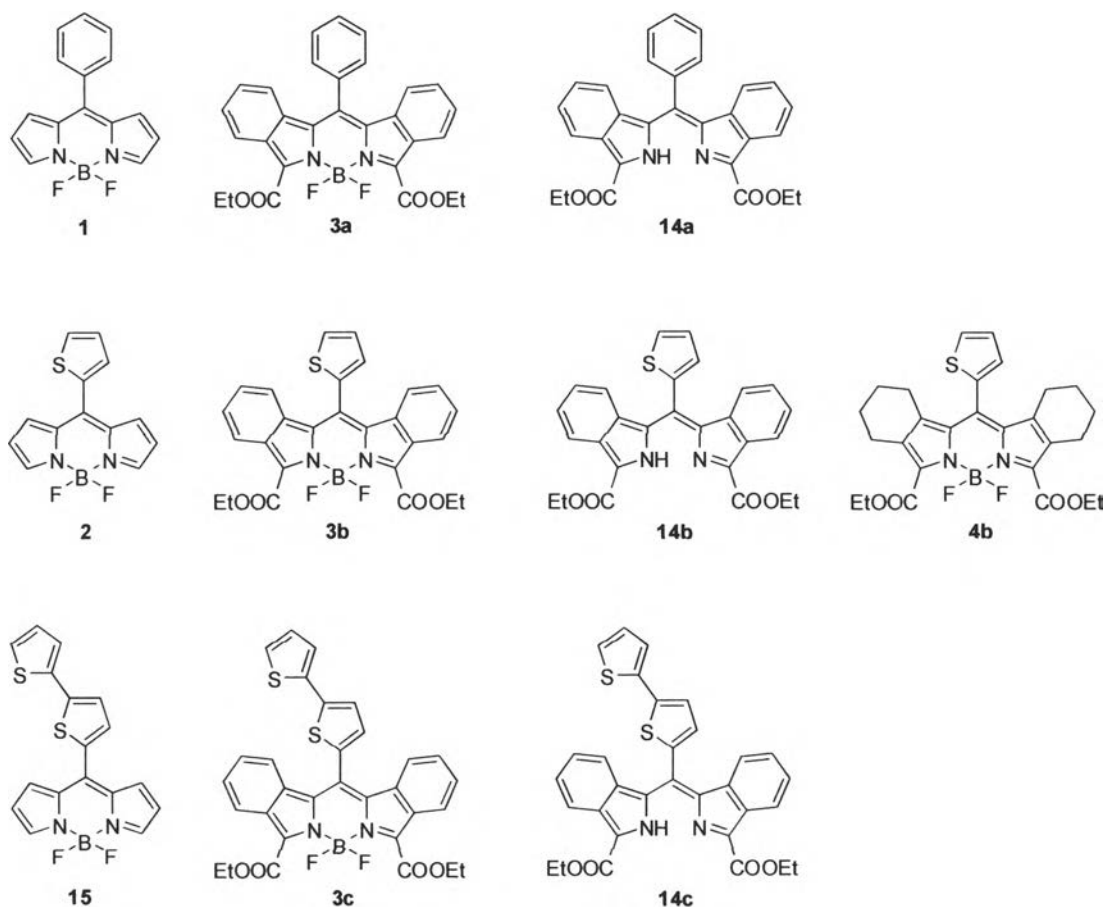


Chart 4-1: Structures of BODIPYs, benzo-BODIPYs, dipyrins and fused-cyclohexenyl BODIPYs synthesized in this work

**Table 4-1:** Spectral properties of BODIPYs **1-4**, dipyrins **14a-c** and BODIPY **15** in toluene at room temperature

Compounds	Absorption wavelength ( $\lambda_{\text{abs}}$ )/nm	$\epsilon \times 10^5$ at $\lambda_{\text{max}}$ ( $\text{M}^{-1} \cdot \text{cm}^{-1}$ )	Emission wavelength ( $\lambda_{\text{em}}$ )/nm	$\Phi_f^a$
<b>1</b>	344, 503	0.5	521	0.05
<b>2</b>	393, 514	0.5	617	0.02
<b>3a</b>	642	1.0	663	0.37
<b>3b</b>	656	0.7	676	0.29
<b>3c</b>	658	0.5	678	0.23
<b>4b</b>	439, 556	0.4	582	0.05
<b>14a</b>	574	0.4	<sup>c</sup> -	<sup>d</sup> -
<b>14b</b>	579	0.3	<sup>c</sup> -	<sup>d</sup> -
<b>14c</b>	589	0.2	<sup>c</sup> -	<sup>d</sup> -
<b>15<sup>b</sup></b>	312, 514	0.3	341, 567	<sup>e</sup> -

<sup>a</sup> Fluorescence quantum yields were calculated by using methylene blue (0.04 in ethanol) as reference [77].

<sup>b</sup> In  $\text{CH}_2\text{Cl}_2$  according to reference [71]

<sup>c</sup> No peak was observed

<sup>d</sup> Value could not be calculated.

<sup>e</sup> Data was not available in reference [71]

Discussion for each spectral properties is given below.

### 4.2.1 UV-Vis absorption spectra

UV/Vis absorption spectra of a solution of BODIPY 1–4 in toluene are shown in Figure 4-1.

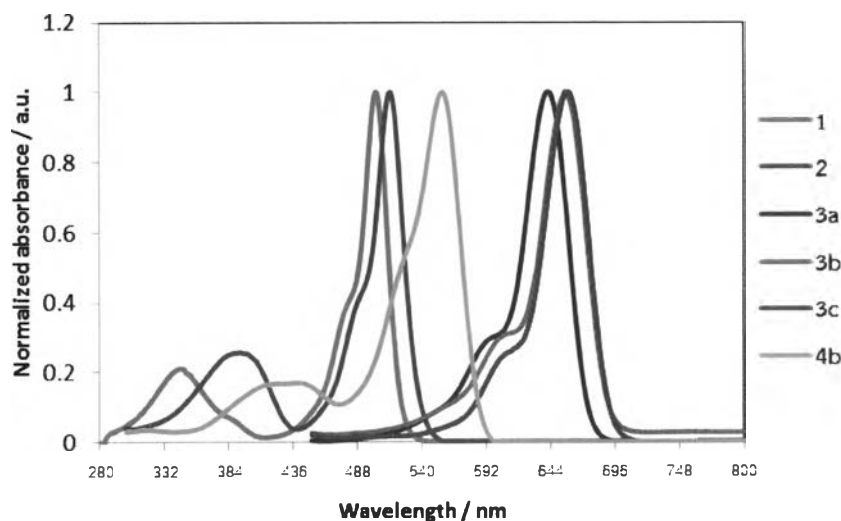


Figure 4-1: Normalized UV-Vis spectra of BODIPYs 1-4

The appearance of two absorption maxima observed in the spectra of BODIPY 1, 2, 4b and 15 can be resulted from one-electron promotion ( $S_0 \rightarrow S_2$ ) at lower wavelength and one-electron HOMO  $\rightarrow$  LUMO transition ( $S_0 \rightarrow S_1$ ) at higher one. In benzo-BODIPY 3a-c, the narrow spectral bands are attributed to two absorption maxima intense  $S_0 \rightarrow S_1$  transition and 0-1 vibrational transition [78, 79]. The benzo-BODIPYs 3a-c were showed a molar absorption coefficient which higher than BODIPY series and BODIPY 4b, therefore the benzo-BODIPYs are suitable for optoelectronic applications.

The effect of the replacement of the meso phenyl group by the meso thienyl one on the absorption characteristics can be seen by the comparison of the absorption maxima of BODIPYs 1 versus 2 and BODIPYs 3a versus 3b. The results showed that the introduction of the thienyl group caused the red-shift of the absorption maxima by 11–14 nm. This is attributed to the smaller steric hindrance caused by the meso-thienyl ring on the BODIPY core compared to that caused by the meso-phenyl group, as there is only one thienyl  $\beta$ -hydrogens that can interact with the pyrrolic  $\beta$ -hydrogen of the BODIPY core, while there are two o-hydrogens on the phenyl ring as explained for the porphyrinic system in the previous studies [80, 81]. Therefore, the meso-thienyl ring can rotate more freely than the meso-



phenyl ring, resulting in the higher  $\pi$ - $\pi$  interaction between the BODIPY and thienyl substituents. However, further extension of the thienyl unit by introducing the second thienyl ring at the thienyl  $\alpha$ -positions of BODIPY **2** and **3b** to give BODIPY **15** and **3c**, respectively, did not significantly affect the absorption maxima of both BODIPYs. The free rotation around the single bond between two thienyl rings and the ring steric hindrance many disturb the pi-pi conjugation system.

The effect of the  $\beta$ -extended  $\pi$ -conjugation of the BODIPYs by fused benzo rings on the absorption characteristics can be seen by the comparison of the absorption maxima of BODIPYs **1** versus **3a**, BODIPYs **2** versus **3b** and BODIPYs **15** versus **3c**. Although the removal of the  $\alpha$ -ester groups on benzo-BODIPYs **3a-c** was not achieved due to the complication of the separation step, the effect of the presence of the  $\alpha$ -ester groups on the physical properties of the BODIPYs was previously reported by Kollmannbergers, M. *et al.* [82]. This study reported about 20 nm red-shift when the  $\alpha$ -ester groups are introduced on their BODIPYs. The results showed that, compared with BODIPYs **1**, **2** and **15**, the introduction of the benzo rings and the  $\alpha$ -ester groups give **3a**, **3b** and **3c**, respectively, caused the red-shift of the absorption maxima by 139–142 nm. The effect of the two fused-cyclohexenyl rings on the absorption characteristics can be seen by the comparison of absorption maxima of BODIPYs **2**, **3b** and **4b**. The results showed that, without the extension of the  $\pi$ -conjugation system, the introduction of the two fused-cyclohexenyl rings on BODIPY **2** caused the small red-shift of the absorption maxima by 42 nm, probably due to the slightly increased rigidity of the molecule caused by the two fused-cyclohexenyl on pyrrolic rings. The extension of the conjugation system on BODIPY **4b** to give BODIPY **3b** caused the further red-shift of the absorption maxima by 100 nm.

The effect of the boron-complexation of dipyrin on the absorption characteristics can be seen by the comparison of the of absorption maxima of dipyrin **14a** versus BODIPY **3a**, dipyrin **14b** versus BODIPY **3b** and dipyrin **14c** versus BODIPY **3c**. UV/Vis absorption spectra of a solution of dipyrins in toluene are shown in Figure 4-2. The results showed that the boron-complexation led to the red-shift of the absorption maxima by 68–77 nm.

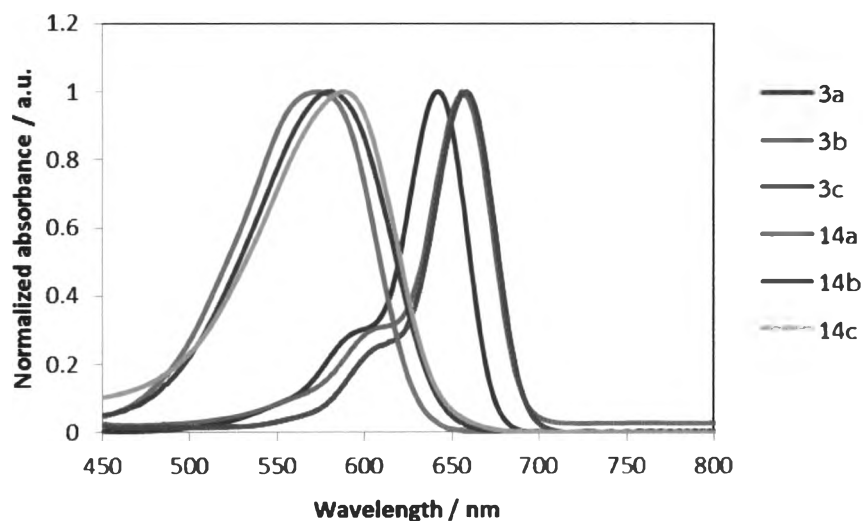
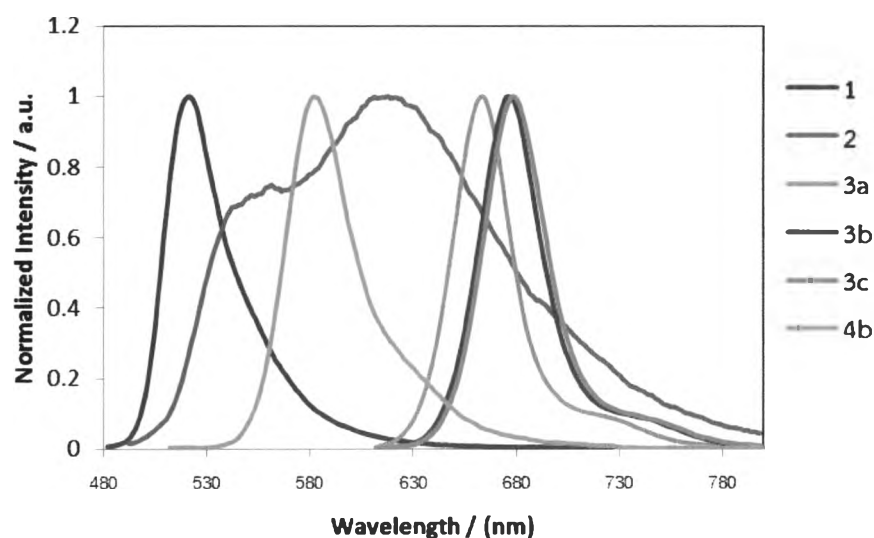


Figure 4-2: Normalized UV-Vis spectra of dipyrins **14a-c** and benzo-BODIPYs **3a-c**

#### 4.2.2 Emission spectra

The emission spectra of BODIPYs **1-4** in solution are shown in **Figure 4-3**. The effect of the replacement of the meso phenyl by the meso thienyl one on the emission characteristics can be seen by the comparison of the emission maxima of BODIPYs **1** versus **2**. The results showed that the introduction of the thienyl group caused the red-shift of the emission maxima by 96 nm. In addition, the effect of the replacement of the meso phenyl by the meso thienyl one on the emission characteristics can be seen by the comparison of the emission maxima of BODIPYs **3a** versus **3b**. The results showed that the introduction of the thienyl group caused the red-shift of the emission maxima by 13 nm. Due to the meso thienyl ring can possibly rotate more freely than the meso phenyl ring, therefore  $\pi$ - $\pi$  interaction between the BODIPY and thienyl substituent can occur than phenyl substituent. The further extension of the thienyl unit by introducing the second thienyl ring at the thienyl  $\alpha$ -positions of BODIPY **3b** to give BODIPY **3c**, respectively, did not significantly affect the emission maxima of both BODIPYs.





**Figure 4-3:** Normalized emission spectra of the solution of BODIPYs 1-4

The effect of the  $\beta$ -extended  $\pi$ -conjugation of BODIPYs by introducing the fused benzo rings on the emission characteristics can be seen by the comparison of the emission maxima of BODIPYs 1 versus 3a, BODIPYs 2 versus 3b and BODIPYs 15 versus 3c. The results showed that, compared with BODIPYs 1, 2 and 15, the introduction of the benzo rings and the  $\alpha$ -ester groups to give 3a, 3b and 3c, respectively, brought about the red-shift of the emission maxima by 59–142 nm. Kollmannberger, M. *et al.* reported the emission red-shift about 21 nm when the  $\alpha$ -ester groups are introduced on their BODIPYs [82]. The effect of the fused-cyclohexyl rings on the emission characteristics can be seen by the comparison of emission maxima of BODIPYs 2, 3b and 4b. The results showed that, the BODIPY 2 was found as a broad signal at 500-800 nm. The introduction of the fused-cyclohexenyl rings on BODIPY 2 to give BODIPY 4b caused narrow of emission compared to the emission of BODIPY 2. This is probably due to the slightly increased rigidity of the molecule caused by the fused-cyclohexenyl ring on pyrrolic rings. The extension of the conjugation system on BODIPY 4b to give BODIPY 3b led to the further red-shift of the emission maxima by 94 nm.



### 4.2.3. Energy gap

The term optical energy gap refers to the energy difference between HOMO to LUMO that can be determined from an intersect of UV absorption and emission spectra as shown in **Figure 4-4** and the following equation [85].

$$\text{Energy gap } (E_{\text{gap}}) = hc / \lambda$$

when  $h = \text{Planks constant} = 6.626 \times 10^{-34} \text{ Joules}\cdot\text{sec}$

$c = \text{speed of light} = 3.0 \times 10^8 \text{ meter/sec}$

$\lambda = \text{intersect wavelength of absorption and emission spectra}$

The estimated optical energy gaps of BODIPYs **1-4** are summarized in **Table 4-2**.

**Table 4-2:** The estimated optical  $E_{\text{gap}}$  from UV spectrometer

BODIPYs	$E_{\text{gap}} / \text{eV}$
<b>1</b>	2.4
<b>2</b>	2.3
<b>3a</b>	1.9
<b>3b</b>	1.8
<b>3c</b>	1.8
<b>4b</b>	2.2

As shown in **Table 4-2**, the BODIPY series and BODIPY **4b** exhibited the energy gaps of 2.3–2.4 eV and 2.2 eV, respectively. The introduction of the fused-cyclohexenyl rings on BODIPY **4b** caused slightly narrower energy gap, probably due to increased rigidity of molecule. The benzo-BODIPY derivatives have energy gap of 1.8–1.9 eV which narrower than the BODIPY series and BODIPY **4b**. This observation indicated that extending the conjugation system of the BODIPYs by introducing the fused rings on the pyrrolic unit can reduce the energy gap of the system.

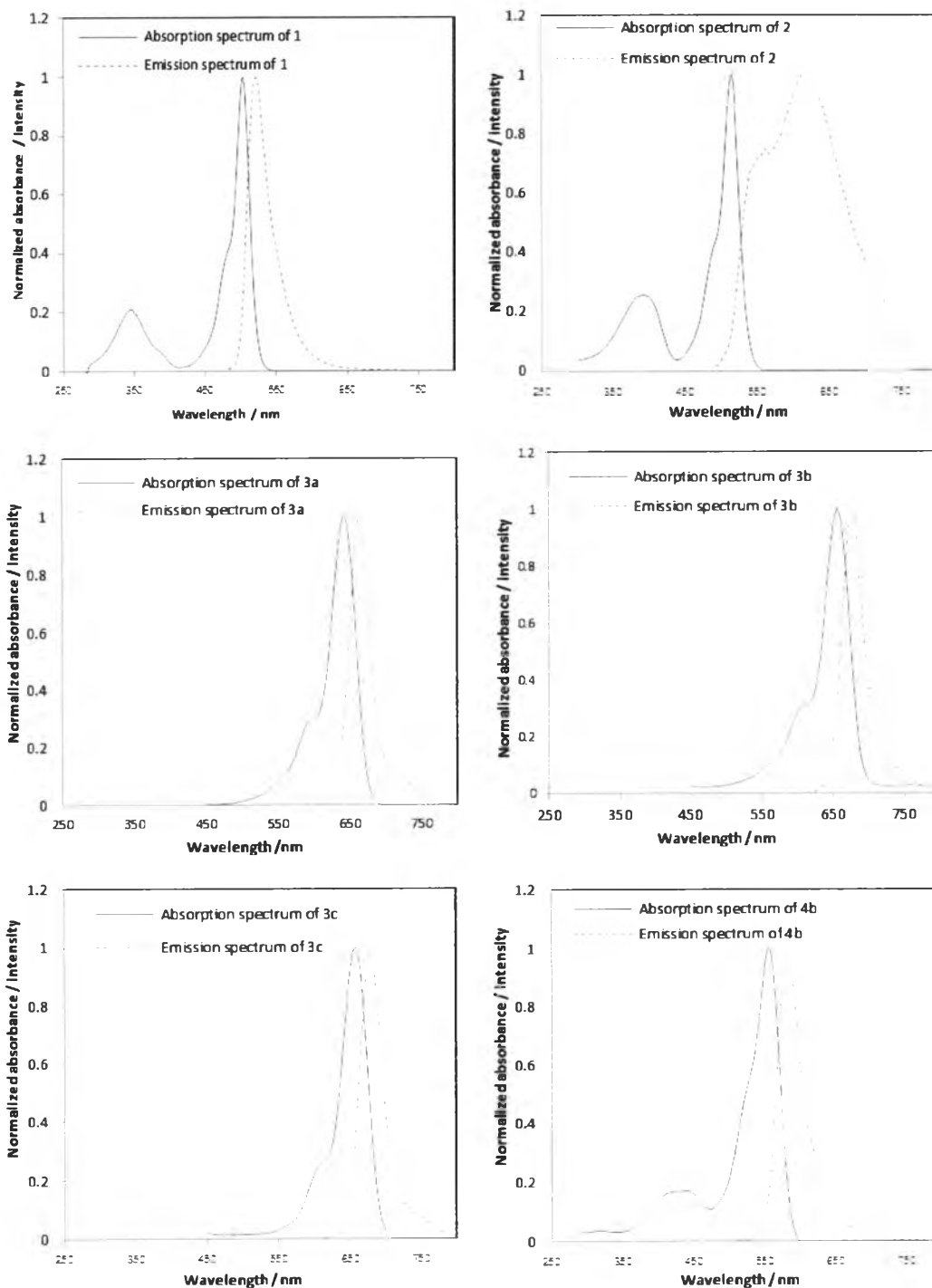


Figure 4-4: Normalized absorption (solid line) and emission (dashed line) spectra of  
(a) BODIPY 1 (b) BODIPY 2 (c) BODIPY 3a (d) BODIPY 3b (e) BODIPY 3c  
(f) BODIPY 4b in toluene



1192222895

#### 4.2.4 Fluorescence quantum yields

As shown in **Table 4-1**, the fluorescence quantum yields of benzo-BODIPYs **3a-c** (0.23–0.44) were found higher than the BODIPYs **1, 2** (0.02–0.05). The fluorescence quantum yield of benzo-BODIPY **3b** was also found to be higher than that BODIPY **4b** (0.29 versus 0.05), indicating the significant effect of the introduction of the benzo-fused structure. The lower fluorescence quantum yields observed for the BODIPYs bearing the meso thienyl group compared to those having the meso phenyl group was probably due to the degree of free rotation of meso substituents [86, 87].

